Acta Cryst. (1976). B32, 539

Crystal Structure and Diffuse X-ray Scattering of the 1·3:2 Salt of 4,4′,5,5′-Tetramethyl-$\Delta^{2,2'}$-bis-1,3-dithiole [TMTTF] and 7,7,8,8-Tetracyano-*p*-quinodimethane [TCNQ], a Nonstoichiometric Quasi One-Dimensional Organic Conductor*

BY THOMAS J. KISTENMACHER, TERRY E. PHILLIPS, DWAINE O. COWAN, JOHN P. FERRARIS† AND AARON N. BLOCH‡
Department of Chemistry, The Johns Hopkins University, Baltimore, Maryland 21218, *U.S.A.*

AND T. O. POEHLER
Johns Hopkins Applied Physics Laboratory, Silver Spring, Maryland 20910, *U.S.A.*

(*Received* 20 *January* 1975; *accepted* 19 *June* 1975)

The diffraction properties of an unusual radical cation–radical anion salt of composition $(TMTTF)_{1\cdot3}(TCNQ)_2$ $[(C_{10}H_{12}S_4)_{1\cdot3}(C_{12}H_4N_4)_2]$ have been studied by single-crystal X-ray methods. The diffraction patterns show a strong subcell of monoclinic symmetry, space group $P2_1/n$, with $a=3\cdot819(1)$, $b=13\cdot021(6)$, $c=34\cdot827(14)$ Å, $\beta=91\cdot68(3)°$, $V=1731\cdot1$ Å^3, $Z=2$ (for the empirical formula 1·3:2), $D_m=1\cdot43(1)$, $D_c=1\cdot433$ g cm^{-3}. Intensities for 2731 reflections with $I>\sigma(I)$ were collected by counter methods in this subcell. The structure was solved by conventional heavy-atom Patterson and Fourier methods and has been refined by full-matrix least-squares calculations to a final R value of 0·127. The final weighted R value and goodness-of-fit are 0·114 and 2·5, respectively. The subcell structure is dominated by homologous columns of cations and anions running parallel to the short a axis. The interplanar spacing in the TCNQ columns is small, 3·24 Å, while the spacing in the TMTTF columns is 3·59 Å and corresponds to about the expected van der Waals separation. Among the columns of molecular cations and anions are channels of TMTTF residues (0·6 per subcell). The end-to-end alignment of the TMTTF residues in these channels approximately parallels the a axis and the stacks of cations and anions. Oscillation photographs about the a axis show a set of diffuse layer lines with a period corresponding to $10/3a$. These are interpreted as arising from an incipient Peierls distortion of the columns, the first observed in an organic system. The material is a semiconductor with a room temperature conductivity of order 10 Ω^{-1} cm^{-1}.

Introduction

The organic charge transfer salt of $\Delta^{2,2'}$-bis-1,3-dithiole (TTF) and 7,7,8,8-tetracyano-*p*-quinodimethane (TCNQ), first developed and studied in these laboratories (Ferraris, Cowan, Walatka & Perlstein, 1973; Bloch, Ferraris, Cowan & Poehler, 1973; Gleiter, Schmidt, Cowan & Ferraris, 1973; Butler, Ferraris, Bloch & Cowan, 1974; Kistenmacher, Phillips & Cowan, 1974; Poehler, Bloch, Ferraris & Cowan, 1974), is the prototype for a class of quasi one-dimensional materials which include the best organic conductors known. The class now contains the TCNQ salts of a sizeable series of analogs and derivatives of TTF (Bloch, Ferraris, Cowan & Poehler, 1973; Ferraris, Poehler, Bloch & Cowan, 1973; Bloch, Cowan & Poehler, 1974; Bechgaard, Bloch & Cowan, 1974; Engler & Patel, 1974). These form almost exclusively in a 1:1 stoichiometry, and their electrical properties exhibit well defined chemical trends (Bloch, 1974; Bloch, Cowan & Poehler, 1974).

Here we report room-temperature X-ray studies on a new TCNQ salt which is unique among the members of the TTF family in several respects. When TMTTF (the tetramethyl derivative of TTF) is combined with TCNQ in solution, crystals may be grown in any of at least three conventional 1:1 phases, one electrically insulating and at least two conducting (Phillips, Ferraris, Kistenmacher, Poehler, Bloch & Cowan, 1974). When the crystals are grown from the vapor phase, however, a new compound appears having the stoichiometry of $(TMTTF)_{1\cdot3}(TCNQ)_2$. Oscillation photographs about the morphologically dominant prismatic axis (a axis and the high conductivity direction) display in addition to the normal Bragg pattern a set of diffuse streaks reminiscent of those arising from the incipient Peierls distortion in the 'mixed valence' platinum chain compounds (Comès, Lambert, Launois & Zeller, 1973; Comès, Lambert & Zeller, 1973). In the context of theoretical discussions of bizarre conduction mechanisms associated with such a distortion (for example, Bardeen 1973; Lee, Rice & Anderson, 1974; Luther & Emery, 1974), it is interesting that $(TMTTF)_{1\cdot3}(TCNQ)_2$ (like the mixed-valence platinum salts) is a semiconductor, with room-temperature conductivity of the order 10 Ω^{-1} cm^{-1}.

The crystal structure of $(TMTTF)_{1\cdot3}(TCNQ)_2$ is itself unusual. The basic structure is not unlike that of (quinolinium) $(TCNQ)_2$ (Kobayashi, Marumo & Saito, 1971) consisting of columns of separately stacked TMTTF and TCNQ radical ions in the ratio

* This investigation was supported by grants from the donors of the Petroleum Research Fund, administered by the American Chemical Society (T.J.K.), and from the Advanced Research Projects Agency, Department of Defense (D.O.C. and A.N.B.).

† Present address: Chemistry Department, University of Texas at Dallas, Richardson, Texas, 75080, U.S.A.

‡ Alfred P. Sloan Foundation Fellow.

1:2. Among the stacks, however, are channels of additional TMTTF molecules whose molecular planes are roughly parallel to the stacking axis. Associated with these molecules is an additional weak superstructure, not commensurate with the period of the diffuse streaks from the columnar stacks.

Experimental

Crystals of $(TMTTF)_{1\cdot3}(TCNQ)_2$ were prepared by the combination of the constituent molecules in the vapor phase (TMTTF/TCNQ ratio equal to 1·09/2, 1 mm of Hg, 180°C). The crystals grow as elongated monoclinic prisms, [100] as the prism axis, with several well developed faces whose normals lie perpendicular to the prism axis.

Preliminary diffraction photographs showed several features: (1) strong layer lines with a periodic repeat length of 3·82 Å; (2) weak layer lines with a repeat length of about 9·6a (36·7 Å); (3) diffuse streaks with a repeat distance of (10/3)a [12·7 Å]. Weissenberg photographs ($0kl$ and $1kl$) for the strong layer lines showed the crystal system of the subcell to be monoclinic, space group $P2_1/n$. Accurate cell dimensions were derived from measurements made on a diffractometer (see below). Attempts were also made to obtain Weissenberg photographs for the weak specular layer lines and the diffuse streaks. We were unsuccessful in obtaining such a photograph for any of the weak specular layer lines, presumably because of the weakness of the diffracted intensities (the weakness of these layer lines also limited the accuracy of measurement of the period of this supercell).

The Weissenberg photograph of a diffuse streak remained completely featureless even after very long (*ca* 4 days) exposures. In the absence of the festoon streaks which would indicate two-dimensional ordering we conclude that the diffraction vectors lie on the diffuse sheets $(h+\frac{1}{3})a^*+\varepsilon b^*+\psi c^*$, where ε and ψ are continuous variables. Hence the corresponding supercell is ordered in one dimension only, with period 10/3a.

An oscillation photograph of the crystal used in data collection is presented in Fig. 1. This crystal was judged to be the best available and was the one crystal for which the full set of weak specular reflections was clear. The diffuse streaks were discernible even on crystals which were considerably less perfect.

The detailed analysis of the crystal structure was performed in the strong subcell. The crystal system is monoclinic with systematic absences ($0k0$, $k=2n+1$; $h0l$, $h+l=2n+1$) which are consistent with the space group $P2_1/n$. Accurate unit-cell dimensions were obtained from a least-squares fit to the 2θ, ω and χ values for 15 carefully centered reflections; the density of the crystals was measured by pycnometric methods in a mixture of carbon tetrachloride and benzene and indicated a stoichiometry of about one TMTTF to two TCNQ with some excess of TMTTF likely. Complete crystal data are given in Table 1.

Table 1. *A comparison of the crystal data for* TTF–TCNQ *and* $(TMTTF)_{1,3}(TCNQ)_2$

TTF–TCNQ*	$(TMTTF)_{1,3}(TCNQ)_2$†
$b=3{\cdot}819$ (2) Å	$a=3{\cdot}819$ (1) Å
$a=12{\cdot}298$ (6)	$b=13{\cdot}021$ (6)
$c=18{\cdot}468$ (8)	$c=34{\cdot}827$ (14)
$\beta=104{\cdot}46$ (4)°	$\beta=91{\cdot}68$ (3)°
$V=839{\cdot}9$ Å^3	$V=1731{\cdot}1$ Å^3
$Z=2$	$Z=2$
$C_{18}H_8N_4S_4$	$(C_{10}H_{12}S_4)_{1\cdot3}(C_{12}H_4N_4)_2$
$D_m=1{\cdot}62$ (1) g cm^{-3}	$D_m=1{\cdot}43$ (1) g cm^{-3}
$D_c=1{\cdot}615$	$D_c=1{\cdot}433$
Space group $P2_1/c$	Space group $P2_1/n$

* Kistenmacher, Phillips & Cowan (1975).
† This study.

A total of 5211 reflections (the hkl, $hk\bar{l}$ quadrant to $2\theta=55°$) were measured on a Syntex $P\bar{1}$ computer-controlled diffractometer; graphite-monochromatized Mo $K\alpha$ radiation was employed. The crystal used in data collection was a monoclinic prism with dimensions $0{\cdot}40\times0{\cdot}10\times0{\cdot}15$ mm; the long axis of the crystal was approximately aligned along the φ axis of the diffractometer. Intensity data were collected by the θ–2θ scan technique; individual scan speeds were determined by a rapid scan at the calculated Bragg peak, and the rate of scanning varied from 2° min^{-1} (less than 100 counts during the rapid scan) to 24° min^{-1} (more than 1000 counts during the rapid scan). Three standard reflections were monitored after every 100 reflections, and their intensities showed no unusual fluctuations over the course of the experiment (maximum deviation of any standard from its mean intensity is about 4%).

The 5211 measured intensities, which included standards and systematic absences as well as some symmetry-related data, were then reduced to a set of 2731 independent reflections with $I>\sigma(I)$. All reflections in this reduced set were assigned observational variances based on the following equation:

$$\sigma^2(I)=S+(B_1+B_2)\,(T_S/2T_B)^2+(pI)^2,$$

where S, B_1 and B_2 are the scan and extremum background counts, T_S and T_B are the scan and individual background counting times ($T_B=\frac{1}{4}T_S$ for all reflections), and p was taken to be 0·03 and represents the expected error proportional to the diffracted beam intensity (Busing & Levy, 1957). The intensities and their associated standard deviations were corrected for Lorentz and polarization effects, but no correction for absorption was applied ($\mu=3{\cdot}8$ cm^{-1}). The intensities were then placed on an approximate absolute scale by the method of Wilson (1942).

Solution and refinement of the structure

A careful examination of a three-dimensional Patterson map allowed the positioning of the two unique sulfur atoms in the TMTTF cation (which is centrosymmetrically distributed about the unit-cell origin).

The positions of the two sulfur atoms were such that a subsequent Fourier map had an approximate mirror plane at $y=0$. Thirteen other heavy atoms, some incorrect, were chosen from this map. A second structure factor Fourier calculation, based now on 15 atoms, allowed the remainder of the heavy atoms to be positioned and the incorrect atoms to be identified. Four cycles of full-matrix, isotropic least-squares refinement, minimizing the quantity $\sum w(|F_o|-|F_c|)^2$ where $w=1/\sigma^2(F_o)$, reduced the R value ($\sum |F_o|-|F_c| / \sum|F_o|$) to 0·31. At this point it was obvious that the geometry of the TMTTF cation (and to a smaller extent the TCNQ anion) was inconsistent with our expectations based on previous results (Kistenmacher, Phillips & Cowan, 1974). A Fourier map computed on the basis of the TCNQ anion alone indicated that the TMTTF cation should be rotated approximately 7° about its plane normal. After the adjustment of the TMTTF cation and four further cycles of refinement, the R value stood at 0·18.

A difference Fourier map was computed at this stage in the analysis, and it showed a channel of residual electron density approaching a maximum value of 2·6 e Å^{-3}. The channel paralleled the a axis and was confined to a region surrounded by two TMTTF cation columns and two TCNQ anion columns. Since the density measurement and analytical chemical data suggested that the correct empirical formula for the compound was $(TMTTF)_{1\cdot3}(TCNQ)_2$ [chemical analysis for $(C_{10}H_{12}S_4)_{1\cdot3}(C_{12}H_4N_4)_2$: calculated: C 59·69; H 3·18; N 15·00, S 22·32%; found: C 59·23, H 3·09, N 14·80, S 22·09%], we attempted to fit three idealized TMTTF molecules* (each with a population factor of 0·10) to the observed channel of residual electron density. An end-to end alignment of three TMTTF molecules along the a axis, with idealized dimensions estimated from the TMTTF cations in the columnar stacks and proper account taken of the contacts between exocyclic methyl groups, requires a unit cell approximately 10 times that of the subcell. This interpretation of the residual electron density is consistent with the analytical chemical data and the weak specular reflections observed on the oscillation photograph. In order to obtain the best fit to the residual electron density, it was necessary to tip two of the TMTTF molecules slightly relative to the ab plane and to assign relatively large temperature factors to the individual atoms. These molecules were also constrained to preserve the centers of symmetry of the averaged subcell.

Four further cycles of least-squares refinement, including in the list of variables anisotropic temperature parameters for the two independent sulfur atoms in the TMTTF cation and the four terminal nitrogen atoms of the TCNQ anion led to a final R value of 0·127. In conjunction with these least-squares cycles, the positions and Eulerian angles of the idealized TMTTF molecules in the channels were periodically adjusted by difference Fourier methods. The final weighted R value ($[\sum w(F_o-F_c)^2/\sum wF_o^2]^{1/2}$) and goodness-of-fit ($[\sum w(F_o-F_c)^2/(NO-NV)]^{1/2}$ where $NO=2731$ independent observations and $NV=123$ parameters) were 0·114 and 2·5, respectively. In the final cycle of refinement, no shift/error exceeded 1·0 for any parameter. A final difference Fourier map showed no peaks exceeding 0·8 e Å^{-3} in the channel of residual density occupied by the TMTTF molecules.

Neutral scattering-factor curves for S, N and C were taken from the compilation of Hanson, Herman, Lea & Skillman (1964). Final atomic parameters for the atoms in the TMTTF cation and the TCNQ anion are collected in Table 2. The final atomic parameters for the atoms in the TMTTF molecules which occupy the channel along the a axis are given in Table 3.*

Table 2. *Coordinates* ($\times 10^4$) *and temperature parameters for the atoms in the* TMTTF *cation and the* TCNQ *anion*

	x	y	z	B
S(1)	−1330 (6)	1207 (1)	400 (0·5)	
S(2)	−1342 (6)	−1019 (1)	469 (0·5)	
C(1)	−2592 (19)	700 (6)	844 (2)	3·27 (14)
C(2)	−2501 (19)	−329 (5)	871 (2)	3·20 (14)
C(3)	−596 (17)	47 (5)	185 (2)	2·95 (12)
C(4)	−3622 (22)	−946 (6)	1218 (2)	4·23 (17)
C(5)	−3590 (21)	1428 (6)	1148 (2)	3·96 (16)
N(1)	4269 (21)	1897 (5)	4032 (2)	
N(2)	4142 (22)	−1430 (6)	4127 (2)	
N(3)	−7971 (21)	1660 (5)	2019 (2)	
N(4)	−8113 (19)	−1668 (5)	2056 (2)	
C(6)	3316 (21)	1152 (6)	3907 (2)	3·81 (15)
C(7)	3260 (21)	−711 (6)	3957 (2)	3·72 (15)
C(8)	2164 (18)	182 (5)	3747 (2)	3·24 (13)
C(9)	173 (17)	134 (5)	3411 (2)	2·83 (12)
C(10)	−915 (18)	−838 (5)	3246 (2)	2·90 (13)
C(11)	−2899 (18)	−882 (5)	2906 (2)	2·85 (13)
C(12)	−3918 (16)	39 (5)	2715 (2)	2·72 (12)
C(13)	−2844 (19)	1016 (5)	2869 (2)	3·14 (14)
C(14)	−833 (19)	1065 (5)	3210 (2)	3·25 (14)
C(15)	−5998 (16)	21 (5)	2379 (2)	2·90 (12)
C(16)	−7087 (20)	931 (6)	2178 (2)	3·38 (14)
C(17)	−7130 (20)	−925 (6)	2201 (2)	3·48 (15)

Anisotropic temperature factors for S(1–2) and N(1–4) defined by the equation $\exp[-(B_{11}h^2+B_{22}k^2+B_{33}l^2+2B_{12}hk+2B_{13}hl+2B_{23}kl)]$. All components have been multiplied by 10^4.

	B_{11}	B_{22}	B_{33}	B_{12}	B_{13}	B_{23}
S(1)	777 (20)	35 (1)	6 (0·2)	6 (4)	5 (1)	0 (0·4)
S(2)	752 (20)	38 (1)	6 (0·2)	−4 (4)	6 (1)	2 (0·4)
N(1)	1325 (87)	55 (5)	12 (1)	−72 (17)	−7 (7)	−8 (2)
N(2)	1153 (84)	74 (6)	12 (1)	15 (17)	−23 (6)	6 (2)
N(3)	1231 (84)	59 (5)	9 (1)	52 (16)	−2 (6)	4 (2)
N(4)	897 (70)	55 (5)	10 (1)	−27 (14)	−20 (5)	−4 (1)

* We have adopted in this paper the following nomenclature: the TMTTF residues in the columnar stacks are referred to as TMTTF *cations*, while the TMTTF moieties in the channels are referred to as *molecules*. No quantitative estimate of the charge on the molecules is available.

* A list of structure factors has been deposited with the British Library Lending Division as Supplementary Publication No. SUP 31220 (18 pp., 1 microfiche). Copies may be obtained through The Executive Secretary, International Union of Crystallography, 13 White Friars, Chester CH1 1NZ, England.

Table 3. *Coordinates* ($\times 10^3$) *and isotropic temperature factors of the atoms in the* TMTTF *molecules*

All atoms have been assigned multiplicities of 0·10.

	x	*y*	*z*	*B* (Å²)
S(21)	260	603	3	7
S(22)	260	382	−8	7
C(21)	667	543	0	7
C(22)	667	442	−5	7
C(23)	18	493	−2	6
C(24)	991	373	−8	8
C(25)	991	612	4	8
S(31)	580	618	8	7
S(32)	580	397	−3	7
C(31)	987	558	5	7
C(32)	987	457	0	7
C(33)	338	507	2	6
C(34)	311	388	−4	8
C(35)	311	627	8	8
S(41)	925	610	7	7
S(42)	925	390	−5	7
C(41)	332	550	4	7
C(42)	332	450	−2	7
C(43)	682	500	1	6
C(44)	656	380	−6	8
C(45)	656	620	8	8

The structure factor and Fourier calculations were carried out with the X-RAY 67 series of programs (Stewart, 1967); the least-squares refinement was carried out employing an extensively modified version of *ORFLS* (Busing, Martin & Levy, 1962); the least-squares planes calculations were performed using the program of Pippy & Ahmed (1968); the illustrations were prepared with the aid of the computer program *ORTEP* (Johnson, 1965). All other calculations were performed with locally written programs.

Discussion of the crystal structure

(*a*) *Molecular geometry of the* TMTTF *cation and the* TCNQ *anion*

Drawings of the TMTTF radical cation and the TCNQ radical anion are shown in Figs. 2 and 3; interatomic distances and angles are also given in these figures. Estimated standard deviations are: S–C 0·007–0·008; C–N 0·009–0·011; C–C 0·010–0·014 Å; bond angles 0·5–0·6°.

The molecular symmetry of the TMTTF radical cation is crystallographically required to be at least $\bar{1}$. Averaged values (*mmm* molecular symmetry) for the TMTTF cation are compared with those for neutral TTF (Cooper, Kenney, Edmonds, Nagel, Wudl & Coppens, 1971; Cooper, Edmonds, Wudl & Coppens, 1974) and the TTF cation in TTF–TCNQ (Kistenmacher, Phillips & Cowan, 1974) in Table 4. Several distinctive trends are observed in the sequence TTF^0 to TTF–TCNQ to $(TMTTF)_{1\cdot3}(TCNQ)_2$: (1) a general increase of about 0·02 Å per step in the bridging carbon–carbon bond [C(3)–C(3)′]; (2) an increase of about the same order of magnitude in the exterior carbon–carbon bond [C(1)–C(2)]; (3) a decrease in the S–C (bridging) distance and an increase in the S–C (exterior) bond. These trends are suggestive of an increase in the amount of charge transfer in the TMTTF cation *versus* the TTF cation in their respective TCNQ salts. This trend is expected since the substitution of the methyl groups in TMTTF for the protons in TTF should result in a decrease in the group ionization potential of the heterofulvalene ring system.

Table 4. *A comparison of the molecular dimensions in the heterofulvalene moieties in* TTF, TTF–TCNQ *and* $(TMTTF)_{1\cdot3}(TCNQ)_2$ *(averaged values, mmm molecular symmetry)*

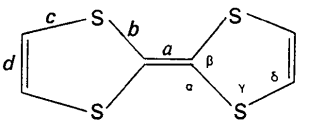

	TTF*	TTF–TCNQ†	$(TMTTF)_{1\cdot3}(TCNQ)_2$‡
a	1·349 (3) Å	1·369 (4) Å	1·385 (14) Å
b	1·757 (2)	1·743 (3)	1·723 (7)
c	1·730 (2)	1·737 (3)	1·747 (7)
d	1·314 (2)	1·323 (3)	1·344 (10)
α	122·8 (2)°	122·7 (2)°	122·4 (6)°
β	114·5 (2)	114·7 (2)	115·2 (5)
γ	94·4 (2)	95·0 (2)	95·8 (6)
δ	118·3 (2)	117·4 (2)	116·6 (6)

* Cooper *et al.* (1971).
† Kistenmacher, Phillips & Cowan (1975).
‡ This study.

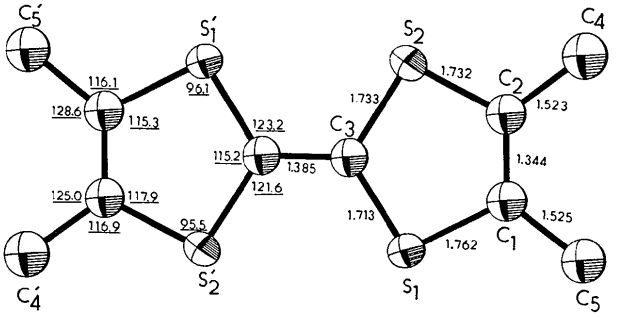

Fig. 2. Interatomic distances and angles in the TMTTF cation. Thermal ellipsoids are drawn at the 50% probability level. Only the sulfur atoms have been refined anisotropically.

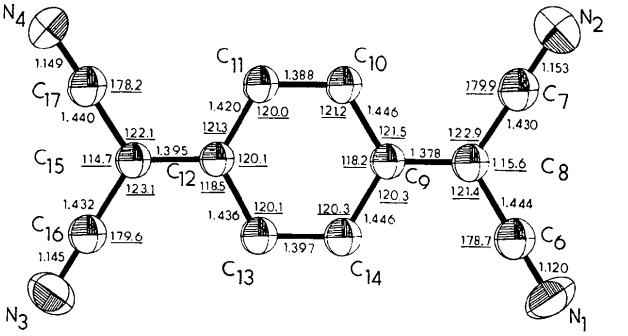

Fig. 3. Interatomic distances and angles in the TCNQ anion. Thermal ellipsoids are drawn at the 50% probability level. The four nitrogen atoms have been refined anisotropically.

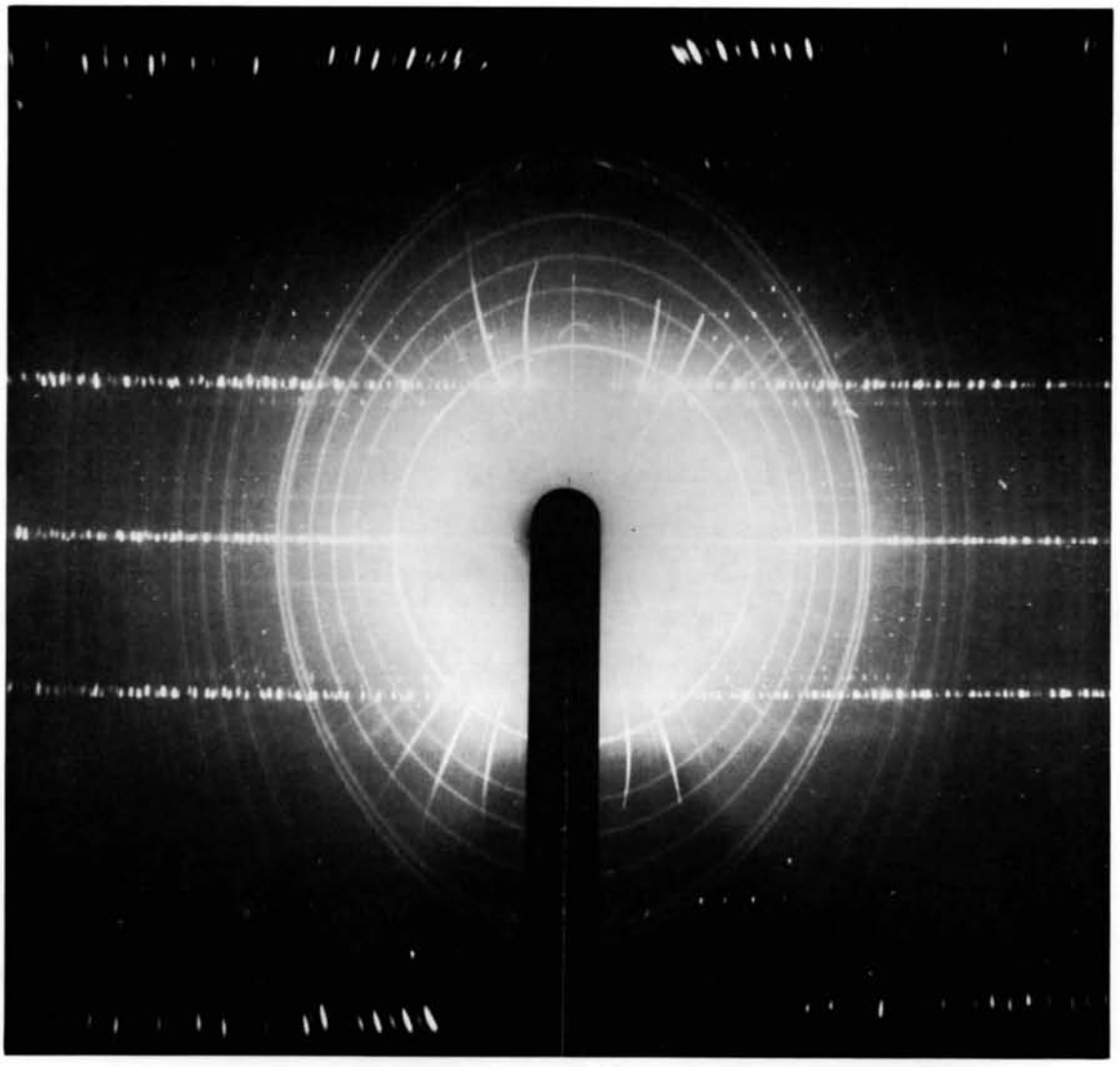

Fig. 1. An oscillation photograph about the *a* axis of the crystal employed in the data collection for $(TMTTF)_{1.3}(TCNQ)_2$. The radiation was nickel-filtered Cu $K\alpha$ with an exposure time of 17·5 h (20° oscillation range). Note the diffuse sheets and the weak specular reflections.

[*To face p.* 542]

A further indication of the increased charge transfer in going from the TTF cation to the TMTTF cation can be found in the degree of planarity of the molecular ions in each case. In both TTF^0 and TTF–TCNQ, the heterofulvalene ring is observed as a slightly distorted chair with each half of the fulvalene ring in an *anti*-envelope conformation. In particular, in TTF^0 and TTF–TCNQ the exterior four-atom plane [S(1), S(2), C(1) and C(2)] and the central plane [S(1), S(2), C(3) and their centrosymmetric mates] fold about the S(1)···S(2) line with dihedral angles of 2·1 (2) and 2·2 (2)°, respectively. The TMTTF cation, however, is more planar (Table 5) with a dihedral angle between the exterior and central planes of only 1·4 (5)°. This increase in the planarity of the TMTTF cation may be attributed to an increase in the aromaticity of the ring system consistent with the bond length trends noted above (aromaticity is expected for a formal +1 charge on the heterofulvalene ring system).

Table 5. *Least-squares planes and the deviations* (Å) *of individual atoms from these planes*

In each of the equations of the planes, the X, Y, and Z are coordinates (Å) referred to the orthogonal axes a, b and c^*. Atoms indicated by an asterisk were given zero weight in calculating the planes; other atoms were weighted equally. Estimated positional uncertainties: S, 0·006; N, 0·024; C, 0·022 Å.

(*a*) TMTTF molecular plane ($-0{\cdot}9408X-0{\cdot}0243Y-0{\cdot}3380Z=0{\cdot}0$ Å)

S(1), S(1′)	+,−0·008	C(1), C(1′)	−,+0·003
S(2), S(2′)	+,−0·008	C(2), C(2′)	−,+0·032
C(3), C(3′)	+,−0·013	C(4), C(4′)	+,−0·015
	C(5), C(5′)	+,−0·002	

(*b*) TMTTF central plane ($-0{\cdot}9388X-0{\cdot}0247Y-0{\cdot}3435Z=0{\cdot}0$ Å)

S(1), S(1′)	−,+0·002	C(1), C(1′)	−,+0·021*
S(2), S(2′)	−,+0·002	C(2), C(2′)	−,+0·051
C(3), C(3′)	+,−0·009	C(4), C(4′)	−,+0·010*
	C(5), C(5′)	−,+0·023*	

(*c*) TMTTF exterior plane ($-0{\cdot}9461X-0{\cdot}0269Y-0{\cdot}3227Z=0{\cdot}0331$ Å)

S(1)	−0·006	C(3)	−0·009*
S(2)	0·006	C(4)	0·058*
C(1)	0·012	C(5)	0·033*
C(2)	−0·012		

(*d*) TCNQ molecular plane ($0{\cdot}8476X-0{\cdot}0383Y-0{\cdot}5292Z=-6{\cdot}5223$ Å)

N(1)	0·032	C(10)	0·007
N(2)	−0·026	C(11)	0·022
N(3)	−0·035	C(12)	0·015
N(4)	0·013	C(13)	0·017
C(6)	0·002	C(14)	0·008
C(7)	−0·020	C(15)	−0·009
C(8)	−0·014	C(16)	−0·019
C(9)	−0·008	C(17)	0·015

(*e*) TCNQ benzenoid ring ($0{\cdot}8520X-0{\cdot}0371Y-0{\cdot}5221Z=-6{\cdot}4411$ Å)

C(9)	−0·006	N(3)	−0·078*
C(10)	0·001	N(4)	−0·034*
C(11)	0·005	C(6)	0·023*
C(12)	−0·007	C(7)	−0·001*
C(13)	0·002	C(8)	−0·000*
C(14)	0·004	C(15)	−0·043*
N(1)	0·059*	C(16)	−0·058*
N(2)	−0·003*	C(17)	−0·026*

The averaged bond angles (Table 4) show some indication of a slight increase in the bond angle at the sulfur atom and a slight increase in the endocyclic bond angle at the exterior carbon atom, while the angles at the bridging carbon remain essentially constant in the sequence TTF^0, TTF–TCNQ to $(TMTTF)_{1\cdot3}(TCNQ)_2$.

The detailed geometry of the TCNQ anion is of interest in light of the attempted correlations between molecular dimensions and the total charge of the ion (Herbstein, 1971; Hoekstra, Spoelder & Vos, 1972; Potworowski & Nyburg, 1975). Because of the relatively small differences in bond lengths and bond angles between $TCNQ^0$ and $TCNQ^{-1}$, and the sensitivity of the geometry to the environment of the molecule, the assignment of charge is not always straightforward. For example, based upon the scale of total molecular lengths established empirically by Potworowski & Nyburg (1975), the charge of the TCNQ anion in $(TMTTF)_{1\cdot3}(TCNQ)_2$ appears to be very close to −0·5. On the other hand, the observed molecular length of 5·620 Å (5·59–5·65 Å for $TCNQ^{-0\cdot5}$) is achieved in an unusual way. In Table 6 we compare the average bond lengths and angles (*mmm* molecular symmetry) for the TCNQ species in $(TMTTF)_{1\cdot3}(TCNQ)_2$ and TTF–TCNQ with those compiled by Herbstein (1971) for $TCNQ^{-1}$ and $TCNQ^{-0\cdot5}$. Whereas for TTF–TCNQ these dimensions suggest a charge between −0·5 and −1·0, consistent with photoemission studies (Butler, Ferraris, Bloch & Cowan, 1974; Grobman, Pollak, Eastman, Maas & Scott, 1974), it is clear that for the 1·3:2 TMTTF salt the geometry of TCNQ is in this context anomalous. In particular, the endocyclic carbon–carbon bond length of 1·393 (10) Å is about 0·04 Å longer, and the exocyclic carbon–carbon bond at least 0·01 Å shorter, than in any of the other cases. We have observed similar anomalies in one of the solution-grown phases of the 1:1 salt TMTTF–TCNQ (Kistenmacher & Phillips, 1974), and also in TMTSF–TCNQ, its selenium analog (Kistenmacher, 1975). We therefore hesitate to make charge assignments for any of these materials on the basis of TCNQ geometry alone.

The TCNQ anion is approximately planar with the expected deviations at the cyano groups (Herbstein, 1971). The six atoms of the benzenoid ring are very planar [plane (*e*), Table 5] and the deviations of the other atoms from this plane indicate some bending plus some twist of the C–$(CN)_2$ planes about the exocyclic C=C bond.

(*b*) *Crystal packing and molecular stacking*

The crystal structure of $(TMTTF)_{1\cdot3}(TCNQ)_2$ is dominated by homologous columns of facially stacked radical cations and radical anions running parallel to

Table 6. *A comparison of the bond lengths* (Å) *and angles* (°) *in* $TCNQ^{-0.5}$, $TCNQ^{-1}$, TTF–TCNQ *and* $(TMTTF)_{1.3}(TCNQ)_2$ *(averaged values, mmm molecular symmetry)*

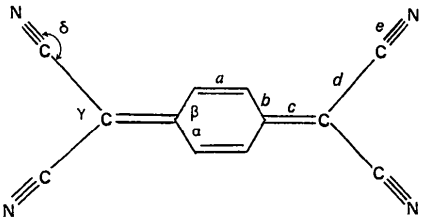

	$TCNQ^{-0.5}$	TTF–TCNQ	$(TMTTF)_{1.3}(TCNQ)_2$	$TCNQ^{-1}$
a	1·354 (2)*	1·356 (3)†	1·393 (10)‡	1·356 (10)*
b	1·434 (2)	1·433 (3)	1·437 (10)	1·425 (7)
c	1·396 (2)	1·402 (3)	1·387 (10)	1·401 (8)
d	1·428 (3)	1·423 (3)	1·437 (10)	1·417 (4)
e	1·17 (1)	1·151 (4)	1·142 (11)	1·15 (1)
α	121·1 (2)	121·4 (2)	120·4 (6)	121·2 (6)
β	117·9 (2)	117·2 (2)	119·2 (6)	117·4 (4)
γ	115·9 (2)	117·8 (2)	115·2 (6)	115·2 (4)
δ	178·5 (2)	177·1 (2)	179·1 (7)	178·6 (6)

* Herbstein (1971).
† Kistenmacher, Phillips & Cowan (1975).
‡ This study.

the short *a* axis. Packing diagrams down the *a**, *b* and $-c^*$ axes are shown in Figs. 4–6. The arrangement of the TMTTF cation columns and TCNQ anion columns is similar to that observed in the structure of (quinolinium) $(TCNQ)_2$ (Kobayashi, Marumo & Saito, 1971). In particular, each column of TMTTF cations is surrounded by six neighboring TCNQ anion columns, while each TCNQ anion column is bounded by three TCNQ anion columns and three TMTTF cation columns (Fig. 5).

The stacking in the TCNQ columns (Fig. 7) is of the 'ring–double-bond' type commonly found in other TCNQ salts (Herbstein, 1971; Shibaeva & Atovmyan, 1972). The interplanar stacking distance at 3·24 Å is about 0·07 Å larger than that found in TTF–TCNQ (3·17 Å, Kistenmacher, Phillips & Cowan, 1974) but is in good agreement with the interplanar spacings for example in (quinolinium) $(TCNQ)_2$ (3·22 Å, Kobayashi *et al.*, 1971) and *N*-methylphenazinium–TCNQ (3·26 Å, Fritchie, 1966).

The molecular stacking in the TMTTF columns (Fig. 8) is similar to that observed in the TTF columns in TTF–TCNQ where the hydrogen atoms on the exterior carbon atoms sit nearly above and below the

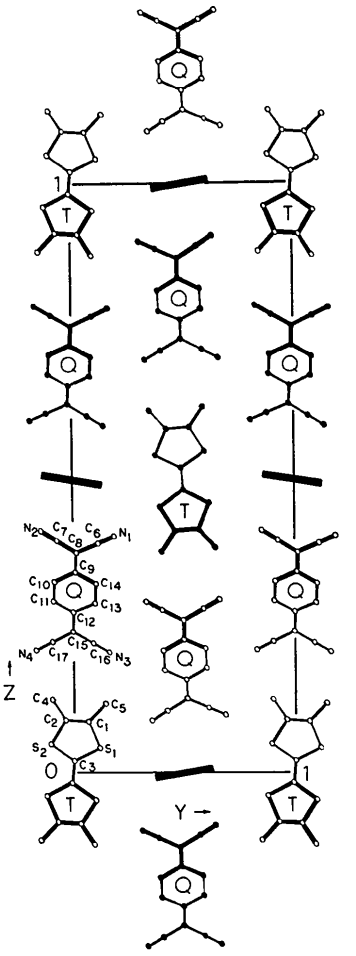

Fig. 4. The crystal packing in $(TMTTF)_{1.3}(TCNQ)_2$ viewed down a*. The unshaded TMTTF cations (T's) have their centroids at $x=0$; the shaded TMTTF cation has its centroid at $x=\frac{1}{2}$. The unshaded TCNQ anions (Q's) have their centroids at about $x=-0{\cdot}2$ ($y=0$) and $-0{\cdot}3$ ($y=\frac{1}{2}$); the shaded TCNQ anions have their centroids at about $x=0{\cdot}2$ ($y=0$) and $0{\cdot}3$ ($y=\frac{1}{2}$). The channels containing the TMTTF molecules are indicated by the solid rectangles.

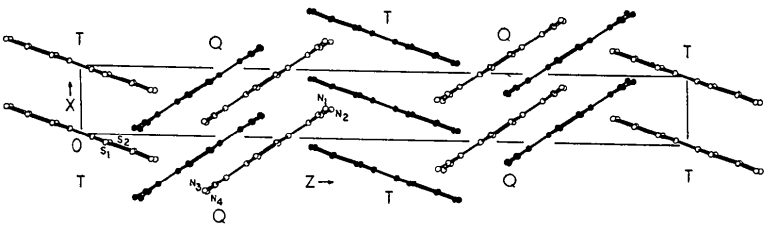

Fig. 5. A view of the crystal packing down the *b* axis. The unshaded TMTTF cations are at $y=0$; the shaded TMTTF cations are at $y=\frac{1}{2}$. The unshaded TCNQ anions are at about $y=0$; the shaded TCNQ anions are at about $y=\frac{1}{2}$. No attempt has been made to show the channels of TMTTF molecules.

S-exterior carbon atom bonds. The slight longitudinal shift in the molecular overlap in the TMTTF columns is probably a result of the repulsion between neighboring exocyclic methyl groups (van der Waals radii of the methyl group being about 2·0 Å: Pauling, 1960). This shift brings the bridging-carbon atoms of alternate molecules into near superposition (Fig. 8). The interplanar spacing in the TMTTF chain of 3·59 Å (compared to a spacing of 3·47 Å in the TTF columns in TTF–TCNQ) is close to the expected value of about 3·5 Å (Herbstein, 1971).

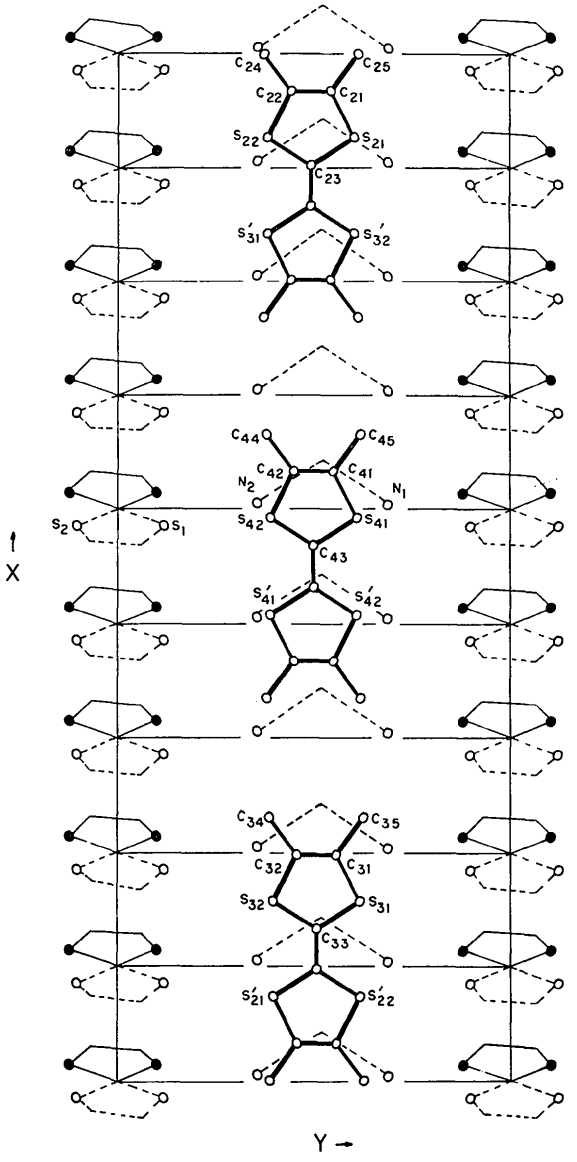

Fig. 6. A view of the columnar crystal packing and the channels of TMTTF molecules. The view direction is $-c^*$. Only the cyano-nitrogen atoms N(1) and N(2) behind the TMTTF molecules have been shown. Illustrations of the TMTTF cations have been placed at the origins of the subcell along the *a* axis (see text).

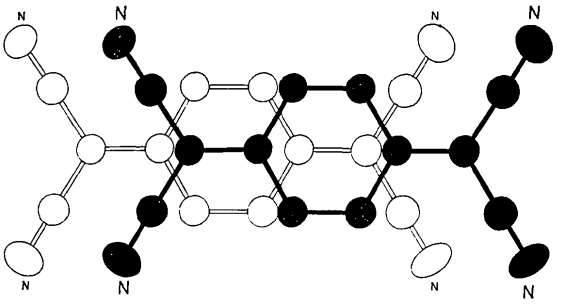

Fig. 7. The molecular overlap in the columnar stacking of the TCNQ anions. The view direction is normal to the molecular planes.

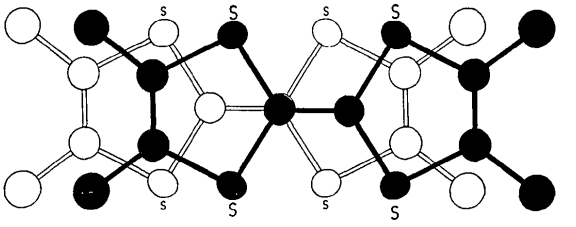

Fig. 8. The molecular overlap in the columnar stacking of the TMTTF cations. The view direction is normal to the molecular planes.

The TMTTF cations and the TCNQ anions are tilted in opposite directions relative to the *bc* plane (Fig. 5) with tilt angles of 19·8 and 32·0°, respectively. The dihedral angle between the TMTTF and TCNQ planes is 51·8° and is comparable with the value observed in TTF–TCNQ, 58·5°, and that in TMTSF–TCNQ, 54·9°. The resulting pseudo-herringbone arrangement of the cations and anions (Fig. 5) is similar to that found in TTF–TCNQ and TMTSF–TCNQ and is in direct contrast to the approximately parallel arrangement of cationic and anionic planes found in (quinolinium) $(TCNQ)_2$ and many other TCNQ salts (Kistenmacher, Phillips & Cowan, 1974).

The TMTTF columns and TCNQ columns in $(TMTTF)_{1\cdot3}(TCNQ)_2$ are more loosely packed than the analogous columns in TTF–TCNQ [the S···N contacts of 3·25 and 3·20 Å which dominate the structure of TTF–TCNQ are replaced in the structure of $(TMTTF)_{1\cdot3}(TCNQ)_2$ by S···N contacts of 3·31 and 3·58 Å, Table 7]. The relative openness of the packing of the columns of cations and anions in $(TMTTF)_{1\cdot3}(TCNQ)_2$ accommodates the channels of TMTTF molecules which run parallel to the *a* axis (Figs. 5 and 6). Each of these channels is surrounded by two cation and two anion columns. The contacts formed by these molecules are mostly with the exocyclic cyano-nitrogen atoms of the TCNQ anions [Table 7(*c*), Fig. 6]. The occasional short N···C contacts [N(1)···C(24) and N(2)···C(25), for example] may indicate small inaccuracies in our model. The slight rotation of each channel about the a^*

axis parallels the rotation of the TCNQ anion columns with which that channel makes the shortest contacts (Fig. 4, Table 7).

Table 7. *A selected list of interatomic contacts* (Å)

(*a*) Stacking contacts less than 3·45 Å in the TCNQ columns

C(6)···C(14)	3·349	C(11)···C(17)	3·347
C(6)···C(9)	3·444	C(12)···C(15)	3·275
C(7)···C(10)	3·381	C(12)···C(17)	3·431
C(8)···C(9)	3·307	C(13)···C(14)	3·307
C(9)···C(12)	3·362	C(13)···C(16)	3·309
C(10)···C(11)	3·315	C(13)···C(15)	3·419

(*b*) Contacts (less than 3·6 Å) involving atoms in the TMTTF columns and the TCNQ columns

S(1)···N(2)[a]	3·577	C(5)···N(3)[c]	3·515
S(2)···N(1)[b]	3·306	C(5)···N(2)[d]	3·562
C(4)···N(1)[b]	3·390	N(3)···C(11)[e]	3·581
C(4)···N(4)[c]	3·555	N(4)···C(13)[f]	3·401
C(5)···N(2)[a]	3·360	N(4)···C(14)[g]	3·453

(*c*) Contacts (less than 3·6 Å) involving the TCNQ nitrogen atoms N(1) and N(2) and the atoms in the TMTTF channels

N(1)···C(24)[h]	3·2	N(2)···S(41)[h]	3·3
N(1)···S(41)[i]	3·3	N(2)···C(32)[i]	3·3
N(1)···C(35)[b]	3·3	N(2)···C(34)[b]	3·3
N(1)···S(42)[h]	3·4	N(2)···C(24)[i]	3·3
N(1)···C(25)[i]	3·4	N(2)···C(31)[h]	3·4
N(1)···S(22)[j]	3·4	N(2)···S(22)[b]	3·4
N(1)···C(44)[h]	3·5	N(2)···S(21)[j]	3·4
N(1)···S(21)[b]	3·5	N(2)···C(21)[h]	3·5
N(1)···C(45)[i]	3·6	N(2)···C(42)[b]	3·5
N(2)···C(25)[h]	3·2	N(2)···C(45)[h]	3·5
N(2)···S(42)[i]	3·3	N(2)···C(23)[j]	3·6
		N(2)···C(23)[b]	3·6

(*d*) Intrachannel contacts in the TMTTF channels

C(24)···C(25′)	3·9	C(34)···C(45′)	4·0
		C(35)···C(44′)	4·0

(*a*)	$\frac{1}{2}-x, \frac{1}{2}+y, \frac{1}{2}-z$	(*f*)	$-\frac{3}{2}-x, -\frac{1}{2}+y, \frac{1}{2}-z$
(*b*)	$\frac{1}{2}-x, -\frac{1}{2}+y, \frac{1}{2}-z$	(*g*)	$-\frac{1}{2}-x, -\frac{1}{2}+y, \frac{1}{2}-z$
(*c*)	x, y, z	(*h*)	$-\frac{1}{2}+x, \frac{1}{2}-y, \frac{1}{2}+z$
(*d*)	$-\frac{1}{2}-x, \frac{1}{2}+y, \frac{1}{2}-z$	(*i*)	$\frac{3}{2}-x, -\frac{1}{2}+y, \frac{1}{2}-z$
(*e*)	$-\frac{3}{2}-x, \frac{1}{2}+y, \frac{1}{2}-z$	(*j*)	$\frac{1}{2}+x, \frac{1}{2}-y, \frac{1}{2}+z$

There have been at least two previous instances in which 'solvent' molecules have been found to occupy open channels in molecular TCNQ structures. In particular, the systems benzidene. TCNQ (Yakushi, Ikemoto & Kuroda, 1974*a*), benzidene.TCNQ.C_6H_6 (Yakushi, Ikemoto & Kuroda, 1974*b*) and benzidene.TCNQ.1·8CH_2Cl_2 (Ikemoto, Chikaishi, Yakushi & Kuroda, 1972) have been studied. In the solvent-free system, mixed stacks of benzidene and TCNQ molecules are close-packed, while in the solvent-containing structures the mixed stacks are found in open, hydrogen-bonded arrays about the channels of solvent molecules. In each of the solvent-containing systems, the solvent channels are bounded by four of the mixed benzidene–TCNQ columns analogous to the four columns (two cationic and two anionic) found in the structure of $(TMTTF)_{1\cdot3}(TCNQ)_2$.

Discussion of the diffuse scattering and the weak specular layer lines

With respect to the 3·82 Å subcell dimension along the *a* axis, the oscillation photograph shows two distinct supercells. One, with period approximately 36·7 Å, is ordered in three dimensions (the weak specular reflections); the other, with period 12·7 Å, is only one-dimensionally ordered (the diffuse streaks). In light of the different periodicities of the supercells (9·6*a* and 10/3*a*), it is natural to associate one superstructure with the channels of TMTTF molecules and the other with the columnar stacks. We have assigned the 36·7 Å period to the true repeat period for the intrachannel species; it is likely then that one or both of the columnar stacks of radical cations and radical anions contain a superstructure of period 10/3*a*.

It is well known that a one-dimensional metallic structure is in principle unstable with respect to a periodic distortion (Peierls, 1955) of twice the Fermi wavenumber k_F. In an array of parallel metallic chains, such a distortion (or the soft phonon which is its dynamic precursor) can give rise to diffuse sheets of scattered X-ray intensity perpendicular to the chain axis, provided that the interchain coupling is sufficiently weak that the phase of the distortion is uncorrelated from chain to chain. Such a pattern has been observed previously in the mixed-valence platinum chain compounds (Comès, Lambert, Launois & Zeller, 1973; Comès, Lambert & Zeller, 1973). To our knowledge, however, the present work represents the first observation of such an effect in an organic material.

Recent approximate band-structure calculations (Berlinsky, Carolan & Weiler, 1974; Lee, Choi & Bloch, 1975) indicate that the intrachain charge-transfer integrals in the TTF and TCNQ columns in TTF–TCNQ are of opposite sign, so that the cation and anion conduction bands have a maximum and a minimum, respectively, at $k=0$. We expect that this conclusion will be general for salts of TCNQ and donors of the TTF family. In conductors of the 1:1 stoichiometry, the result is that the two conduction bands must cross at the Fermi level where the interchain coupling opens an energy gap over most of the Brillouin zone. The one-electron band structure is therefore that of a very weak semimetal, and tends to suppress the Peierls instability (Cohen, Hertz, Horn & Shante, 1974).

In contrast, the 1·3:2 stoichiometry in $(TMTTF)_{1\cdot3}(TCNQ)_2$ lifts the constraint that the band crossing take place at the Fermi level, and the instability is stronger. The distortion will be most favorable for charge transfers such that be cation and anion Fermi wavelengths are commensurate, as for $TMTTF^{+1\cdot2}(TCNQ^{-0\cdot6})_2.0\cdot3TMTTF^0$ or $TMTTF^{+0\cdot6}(TCNQ^{-0\cdot6})_2.0\cdot3TMTTF^{+2}$. From the weak interchain coupling implied by the long S···N contacts (Table 7), we infer that the three-dimensional ordering temper-

ature (Lee, Rice & Anderson, 1974) may be particularly low.

Clearly, low-temperature X-ray and inelastic neutron diffraction studies are required to determine the validity of our identification of the diffuse streaks with a Peierls distortion. At present such experiments are severely inhibited by the limited size and quality of the crystals available.

Note added in proof: – While this manuscript was in the press, Denoyer, Comès, Garito & Heeger (1975) and Kagoshima, Anzai, Kajimura & Ishigura (1975) independently reported weak diffuse X-ray scattering arising from a Peierls distortion in TTF–TCNQ below 53 K.

References

BARDEEN, J. (1973). *Solid State Commun.* **13**, 357–359.

BECHGAARD, K., BLOCH, A. N. & COWAN, D. O. (1974). *Chem. Commun.* pp. 937–938.

BERLINSKY, A. J., CAROLAN, J. F. & WEILER, L. (1974). *Solid State Commun.* **15**, 795–801.

BLESSING, R. H. & COPPENS, P. (1974). *Solid State Commun.* **15**, 215–221.

BLOCH, A. N. (1974). In *Energy and Charge Transfer in Organic Semiconductors*, edited by K. MASUDA and M. SILVER, pp. 159–166. New York: Plenum.

BLOCH, A. N., COWAN, D. O. & POEHLER, T. O. (1974). In *Energy and Charge Transfer in Organic Semiconductors*, edited by K. MASUDA and M. SILVER, pp. 167–174. New York: Plenum.

BLOCH, A. N., FERRARIS, J. P., COWAN, D. O. & POEHLER, T. O. (1973). *Solid State Commun.* **13**, 753–757.

BUSING, W. R. & LEVY, H. A. (1957). *J. Chem. Phys.* **26**, 563–568.

BUSING, W. R., MARTIN, K. O. & LEVY, H. A. (1962). *ORFLS*. Oak Ridge National Laboratory Report ORNL-TM-305.

BUTLER, M. A., FERRARIS, J. P., BLOCH, A. N. & COWAN, D. O. (1974). *Chem. Phys. Lett.* **24**, 600–602.

COHEN, M. H., HERTZ, J., HORN, P. M. & SHANTE, V. K. S. (1974). *Int. J. Quant. Chem. Symp.* No. 8, pp. 491–498.

COMÈS, R., LAMBERT, M., LAUNOIS, H. & ZELLER, H. R. (1973). *Phys. Rev.* B**8**, 571–575.

COMÈS, R., LAMBERT, N. & ZELLER, H. R. (1973). *Phys. Stat. Sol.* B**58**, 587–592.

COOPER, W. F., EDMONDS, J. W., WUDL, F. & COPPENS, P. (1974). *Cryst. Struct. Commun.* **3**, 23–26.

COOPER, W. F., KENNEY, N. C., EDMONDS, J. W., NAGEL, A., WUDL, F. & COPPENS, P. (1971). *Chem. Commun.* pp. 889–890.

DENOYER, F., COMÈS, F., GARITO, A. F. & HEEGER, A. J. (1975). *Phys. Rev. Lett.* **35**, 445–448.

ENGLER, E. & PATEL, V. (1974). *J. Amer. Chem. Soc.* **96**, 7377–7378.

FERRARIS, J., COWAN, D. O., WALATKA, V. & PERLSTEIN, J. (1973). *J. Amer. Chem. Soc.* **95**, 948–949.

FERRARIS, J. P., POEHLER, T. O., BLOCH, A. N. & COWAN, D. O. (1973). *Tetrahedron Lett.* **27**, 2552–2556.

FRITCHIE, C. J. (1966). *Acta Cryst.* **20**, 892–898.

GLEITER, R., SCHMIDT, E., COWAN, D. & FERRARIS, J. (1973). *J. Electron Spectrosc. Relat. Phenom.* **2**, 207–210.

GROBMAN, W. D., POLLAK, R. A., EASTMAN, D. E., MAAS, E. T. & SCOTT, B. A. (1974). *Phys. Rev. Lett.* **32**, 534–537.

HANSON, H. P., HERMAN, F., LEA, J. D. & SKILLMAN, S. (1964). *Acta Cryst.* **17**, 1040–1044.

HERBSTEIN, F. H. (1971). *Perspect. Struct. Chem.* **4**, 166–395.

HOEKSTRA, A., SPOELDER, T. & VOS, A. (1972). *Acta Cryst.* B**28**, 14–25.

IKEMOTO, I., CHIKAISHI, K., YAKUSHI, K. & KURODA, H. (1972). *Acta Cryst.* B**28**, 3502–3506.

JOHNSON, C. K. (1965). *ORTEP*. Oak Ridge National Laboratory Report ORNL-3794.

KAGOSHIMA, S., ANZAI, H., KAJIMURA, K. & ISHIGORA, T. (1975). *J. Phys. Soc. Japan*, **39**.

KISTENMACHER, T. J. (1975). To be published.

KISTENMACHER, T. J. & PHILLIPS, T. E. (1975). To be published.

KISTENMACHER, T. J., PHILLIPS, T. E. & COWAN, D. O. (1974). *Acta Cryst.* B**30**, 763–767.

KOBAYASHI, H., MARUMO, F. & SAITO, Y. (1971). *Acta Cryst.* B**27**, 373–378.

LEE, P. A., RICE, T. M. & ANDERSON, P. W. (1974). *Solid State Commun.* **14**, 703–709.

LEE, W. T., CHOI, S. & BLOCH, A. N. (1975). To be published.

LUTHER, A. & EMERY, V. J. (1974). *Phys. Rev. Lett.* **33**, 589–592.

PAULING, L. (1960). *The Nature of the Chemical Bond*, 3rd ed. Ithaca: Cornell Univ. Press.

PEIERLS, R. E. (1955). *Quantum Theory of Solids*. Oxford Univ. Press.

PHILLIPS, T. E., FERRARIS, J. P., KISTENMACHER, T. J., POEHLER, T. O., BLOCH, A. N. & COWAN, D. O. (1974). Unpublished work.

PIPPY, M. E. & AHMED, F. R. (1968). NRC Crystallographic Programs, National Research Council, Ottawa, Canada.

POEHLER, T. O., BLOCH, A. N., FERRARIS, J. P. & COWAN, D. O. (1974). *Solid State Commun.* **15**, 337–340.

POTWOROWSKI, J. A. & NYBURG, S. C. (1975). To be published.

SHIBAEVA, R. P. & ATOVMYAN, L. O. (1972). *J. Struct. Chem.* **13**, 514–531.

STEWART, J. M. (1967). X-RAY 67. Tech. Rep. 67–58, Comput. Sci. Center, Univ. of Maryland, College Park, Maryland.

WILSON, A. J. C. (1942). *Nature, Lond.* **150**, 152.

YAKUSHI, K., IKEMOTO, I. & KURODA, H. (1974*a*). *Acta Cryst.* B**30**, 835–837.

YAKUSHI, K., IKEMOTO, I. & KURODA, H. (1974*b*). *Acta Cryst.* B**30**, 1738–1742.